JACS
JOURNAL OF THE AMERICAN CHEMICAL SOCIETY

COMMUNICATION

pubs.acs.org/JACS

Photo-Cross-Linking-Assisted Thermal Stability of DNA Origami Structures and Its Application for Higher-Temperature Self-Assembly

Arivazhagan Rajendran,[†,‡] Masayuki Endo,[*,‡,§] Yousuke Katsuda,[†] Kumi Hidaka,[†] and Hiroshi Sugiyama[*,†,‡,§]

[†]Department of Chemistry, Graduate School of Science, Kyoto University, Kitashirakawa-oiwakecho, Sakyo-ku, Kyoto 606-8502, Japan
[‡]CREST, Japan Science and Technology Corporation (JST), Sanbancho, Chiyoda-ku, Tokyo 102-0075, Japan
[§]Institute for Integrated Cell-Material Sciences (iCeMS), Kyoto University, Yoshida-ushinomiyacho, Sakyo-ku, Kyoto 606-8501, Japan

Supporting Information

ABSTRACT: Heat tolerance of DNA origami structures has been improved about 30 °C by photo-cross-linking of 8-methoxypsoralen. To demonstrate one of its applications, the cross-linked origami were used for higher-temperature self-assembly, which markedly increased the yield of the assembled product when compared to the self-assembly of non-cross-linked origami at lower-temperature. By contrast, at higher-temperature annealing, native non-cross-linked tiles did not self-assemble to yield the desired product; however, they formed a nonspecific broken structure.

Structural DNA nanotechnology has attracted much attention since the recent development of the "scaffolded DNA origami" method by Rothemund.[1] This method is highly flexible and can be used to create a variety of two- and three-dimensional structures of defined size.[2] They can also be self-assembled to create larger structures.[3] The nanostructures prepared by this method have been used for many applications such as a platform for the nanopatterning of a variety of functional molecules,[4] templates for the growth of nanowires,[5] as nanochip in solution to monitor biochemical reactions[6] and conformational changes,[7] and for single molecular analysis of various functionalities.[8] The origami structures can also be confined within a lithographically patterned surface for nanoscale electronic and photonic applications.[9] However, these structures can be used only at low-temperatures of ∼55 °C or less in solution,[10] because they melt beyond this temperature. This is a major disadvantage of materials prepared using DNA, and this problem must be resolved as most practical devices require greater temperature resistance. In addition, they should be inert to the repeated thermal changes that may be required for the stepwise assembly of origami tiles themselves or functional molecules on the origami structures. Hence, new strategies to increase the thermal stability of the DNA origami nanostructures are required. The origami tiles retain their structure and remain folded in cell lysate[11] and against nuclease digestion.[10] However, there is no report on the thermal stability of these structures at temperatures over 55 °C.

Enzymatic[12] and photoligation[13] have been applied in molecular biology and DNA nanotechnology for this purpose. The former has serious disadvantages because it requires an enzyme that is sensitive to the buffer condition, and effective ligation is difficult in an extremely tight space where no enzyme can gain access. The latter method of photoligation is relatively better, because it offers efficient ligation in a condition in which the nanostructures are prepared. Despite the advantages, photoligation requires modified DNAs that are synthetically too laborious, particularly for the origami method, which uses more than 200 staple strands. The better way to overcome these drawbacks is to use a cross-linker that can penetrate easily into the double helix and can bind covalently and irreversibly to both strands of the DNA. Cross-linkers are known to stabilize the nucleic acids[14] and are expected to increase the thermal stability of the origami nanostructures. Here, we report on the photo-cross-linking of DNA origami using 8-methoxypsoralen (8-MOP), which increases the thermal stability of the origami structures. We also describe one of its applications for the self-assembly of these structures at higher-temperature. 8-MOP is a naturally occurring drug that is present in a variety of vegetables. In the presence of ultraviolet (UV) light, it forms covalent adducts with pyrimidine bases in nucleic acids (Figure 1c).[15] Studies on 8-MOP are rapidly growing as the combination of 8-MOP with UVA irradiation (PUVA therapy) is a standard treatment for various dermatoses like vitiligo and psoriasis.[16]

In this study, we have adopted our previous jigsaw-shaped origami tiles.[17] Scheme of a model tile, monomer tiles used in this study, structure of the 8-MOP, general photo-cross-linking scheme and the desired product of the self-assembly are shown in Figure 1. The mechanism of the photo-cross-linking can be found elsewhere.[18] The detailed designs of the tiles are given in Supporting Information (SI, Figure S1). The origami tiles were prepared by mixing the M13mp18 viral DNA and staple strands in Tris-HCl buffer (pH 7.6) containing Mg^{2+} and EDTA. After annealing from 85 to 15 °C at a rate of −1.0 °C/min, the excess staples were removed by gel filtration. In the absence of 8-MOP, tile-0 was incubated at 58 or 60 °C for 1 h and then cooled rapidly on ice. The purpose of this experiment was to study whether the origami structures remain folded at these temperatures. The melted tile-0 was visualized by atomic force microscopy (AFM, Figure 2a) image which shows that the origami structures are not stable at 60 °C. However, nearly half of the tiles were melted at 58 °C (SI, Figure S2), indicating that the melting point lies around this temperature. Note that the stability of the origami is related to the length of the staple strands. Most of the staples used in this study were 32-mer, and hence, the stabilities reported here are associated with this length.

Received: May 18, 2011
Published: August 22, 2011

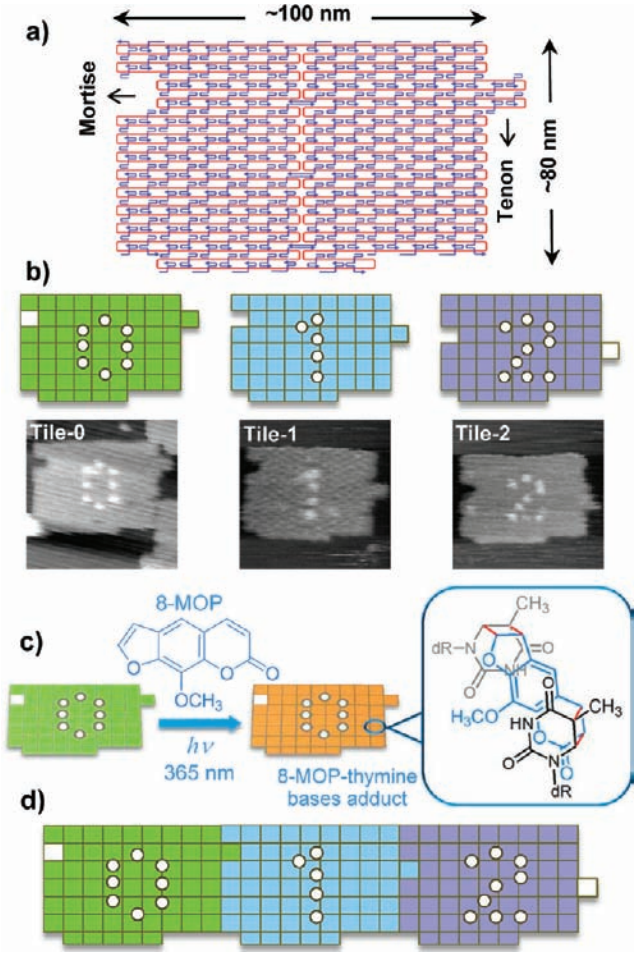

Figure 1. (a) Scheme of an origami tile showing the tenon and mortise. (b) The monomer origami tiles represented as a matrix of blocks and their AFM images. One block represents four 32-mer duplexes. (c) The structure of 8-MOP, scheme of photo-cross-linking and an adduct formed between 8-MOP (light blue) and thymine bases (gray and black). The cross-linking is denoted by red lines. (d) Schematic drawing of the desired self-assembled product. AFM images correspond to a size of 160 × 160 nm.

Next, we tried to optimize the irradiation time for efficient cross-linking. The purified solution of tile-0 was divided into several portions and 8-MOP was added to each solution at a final concentration of 500 μM. The individual solutions were kept on ice and irradiated with 365 nm light for 1, 5, 10, 30, 45, 60, and 90 min. After irradiation, each solution was subdivided into two portions, one of which was incubated at 60 °C and the other at 70 °C for 1 h. The resulting structures were frozen by rapid cooling on ice and imaged using AFM. The structure was not damaged by the irradiation time of 1 h (Figure 2b,c), whereas shorter or longer irradiation times caused complete breakage of the structure (see SI, Figure S2). A shorter irradiation time may not be sufficient for the completion of the cross-linking, and prolonged UV exposure may damage the DNA. It is noteworthy that the photo-cross-linking of origami requires such a long time. It could be possibly due to the rigid and tightly packed nature of the origami structure and its nanomolar concentration.

We extended our studies of the incubation temperature to 80, 85, and 90 °C for the optimum irradiation time of 1 h. Surprisingly, the tiles retained their folded structure even at 80 and 85 °C

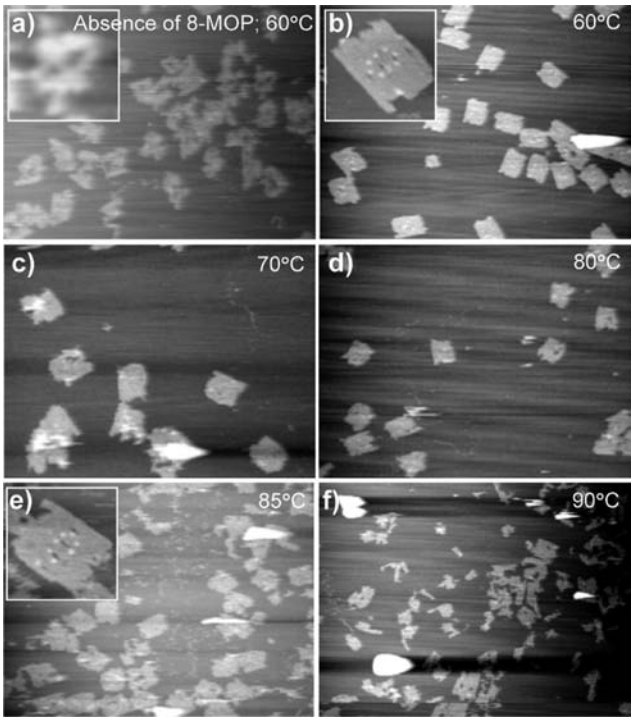

Figure 2. (a) AFM image of tile-0 after incubation at 60 °C for 1 h in the absence of 8-MOP. (b–f) AFM images of tile-0 cross-linked with 8-MOP (500 μM, 1 h irradiation) and after 1 h incubation at 60, 70, 80, 85, and 90 °C, respectively. Insets are the zoom-in images of tile-0. Image sizes: 1400 × 1050 nm (zoom-out) and 170 × 170 nm (insets).

(Figure 2d,e). At 90 °C, most of the tiles were broken, leaving only few well-formed tiles (Figure 2f). The solution-state melting point of the cross-linked origami was expected to lie between 85 and 90 °C, which is ~30 °C increase when compared to the non-cross-linked structure. Similarly, the concentration of 8-MOP was optimized by keeping constant irradiation time of 1 h and 10 nM of M13 strand. The optimum concentration was in the range of 250–500 μM (SI, Figure S3). Although this concentration seems to be high for the cross-linking experiments, it may be necessary for the origami structure with ~7.25 kbp. The melting temperatures estimated by AFM analysis are further confirmed by the UV-melting analysis (see SI, Figure S4). The irreversible nature of the cross-linker plays a vital role in stabilizing the origami structures. This is confirmed by the reversible cross-linking of bisquinone methide–acridine conjugate (bisQMP).[19] The tiles cross-linked with bisQMP failed to retain the folded structure at temperature as low as 60 °C (SI, Figure S5), suggesting that the reversible cross-linking may not provide heat tolerance to the origami structures. Note, the formation of the noncovalent interactions, monoadducts, and cross-linking was found to be 26, 14 and 60%, respectively, for deoxyoligonucleotides with 8-MOP as estimated by infrared multiphoton dissociation (IRMPD)-mass spectroscopy (MS).[20] We anticipate that the origami structures may also display a similar cross-linking yield.

To demonstrate a representative application of the cross-linking-driven thermal stability, one-dimensional self-assembly of the tiles was performed at 60 °C, the temperature at which the non-cross-linked tiles were found to melt. Three different tiles were used for this purpose; each differ in the position of the tenon and mortise, and the numbers (0, 1, and 2 displayed by

dx.doi.org/10.1021/ja204546h |J. Am. Chem. Soc. 2011, 133, 14488–14491

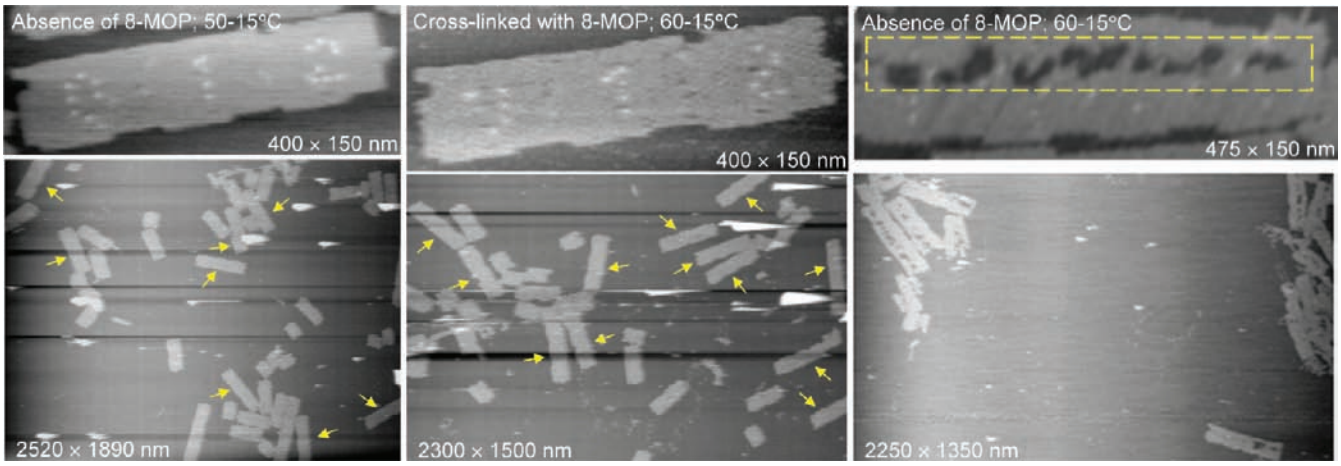

Figure 3. (Left) AFM images of the self-assembled product after low-temperature annealing from 50 to 15 °C and in the absence of 8-MOP. (Middle) AFM images after higher-temperature (60−15 °C) self-assembly of the photo-cross-linked tiles. (Right) Images after higher-temperature self-assembly of non-cross-linked tiles. In all the cases, annealing rate was set to be −0.05 °C/min and the non-cross-linked connecting strands were added during the self-assembly. The arrows denote the well formed trimers and the dotted rectangle indicate the broken part of the structure. The image size is given at the bottom of each image.

tile-0, tile-1 and tile-2, respectively) by hairpin strands. A schematic drawing of the desired self-assembled product is shown in Figure 1d. The tenons and mortises that are involved in the connection during the self-assembly possess two connecting staples each. In addition, there are three connecting staples per side were kept along the corners that involved in assembly. No connecting strand was kept at the tenon, mortise, and corners that are not involved in the assembly (the mortise and left corner in tile-0, and the tenon and right corner of tile-2). Part of a connecting strand was designed to base pair with the M13 in a tile, leaving an overhang region of eight bases. During self-assembly, the overhang region will be hybridized directly to the M13 in the neighboring tile so that the connecting strand will bridge an intermolecular scaffold seam between origami monomers. Each tile was prepared and purified separately, and used for further studies. From this point, the optimized conditions of 1 h irradiation and 500 μM of 8-MOP were used for the cross-linking experiments.

The self-assembly was performed in two different ways: (i) the connecting strands were added separately during the self-assembly of the 8-MOP cross-linked tiles; and (ii) the connecting strands were added during the monomer tile formation and thus were present within the tile. Because the connecting strands were added during the self-assembly, they were non-cross-linked in the former case, whereas they were cross-linked at the duplex regions and form monoadducts at the overhang regions in the latter method as they were placed within the tile. In the first method, the purified tiles were mixed together at an equimolar concentration, 4 times excess concentration of the connecting strands was added, and the lower-temperature self-assembly was carried out from 50 to 15 °C at a rate of −0.05 °C/min in the absence of 8-MOP. The assembled product was analyzed using AFM imaging as shown in Figure 3 (left). The self-assembly successfully resulted in the trimer as designed. The yield was ∼40% (60 tiles were counted), which is comparable to our previous result.[17] In a parallel experiment, 8-MOP was added to the purified tiles and irradiated with UVA light. After irradiation, the higher-temperature self-assembly was performed from 60 to 15 °C at the same cooling rate. The self-assembly was successful (Figure 3, middle), and interestingly, the yield was increased to ∼61% (59 tiles were counted; also see SI, Figure S6). The yield increase in the presence of cross-linker might be due to the higher-temperature annealing where the hybridization of the connecting strands might be more efficient when compared to the lower-temperature. As a control experiment, the same assembly was executed under identical conditions and in the absence of a cross-linker and photoirradiation. In this case, the self-assembly was not successful, while a broken structure was observed (Figure 3, right). This could be due to the melting of the tiles at 60 °C in the absence of 8-MOP, which does not permit the desired self-assembly while leading to a nonspecific broken structure by reannealing the melted origami upon slow cooling of −0.05 °C/min. Moreover, the damage in the structure was found only near the tenons and mortises (indicated by the dotted rectangle in Figure 3) where the staples differ between tiles. However, no damage was found at the positions where the staples had identical sequences in all the tiles (see SI, Figure S1 for the details of the tile design).

We have also carried out the self-assembly by following the second method, that is, by adding the connecting strands during the tile formation. The excess staples and the connecting strands were removed after tile preparation. The low-temperature self-assembly of the non-cross-linked tiles resulted the trimers with a slightly lower yield of ∼36% (67 tiles were counted, Figure S7a). Next, the higher-temperature self-assembly of the cross-linked tiles was carried out. Surprisingly, the product yield was decreased to ∼15% (40 tiles were counted, Figure S7b). Here, the connecting strands were placed within the tiles with a single-stranded overhang, and thus, the overhang regions form monoadducts during the photoirradiation. The single-stranded regions of the M13, which are complementary to the overhang regions, also formed the monoadducts. Thus, the base pairing during the self-assembly may be impeded because of double monoadducts (one from the M13 and the other from the overhang region), and this could have decreased the product yield, as observed. However, in the previous method, the connecting strands were free from 8-MOP as mentioned above, which would favor the base pairing between the monoadducts of M13 regions and 8-MOP

dx.doi.org/10.1021/ja204546h |J. Am. Chem. Soc. 2011, 133, 14488–14491

free connecting strands. Higher-temperature self-assembly of the non-cross-linked tiles again resulted the broken structure (Figure S7c).

In conclusion, we have improved the heat resistance of the origami structures up to 30 °C in solution by photo-cross-linking with 8-MOP. We believe that the cross-linked structures may have even better stability when surface immobilized or confined in the lithographically patterned surface. To show a representative application of the heat resistance, we performed higher-temperature self-assembly of the cross-linked origami structures, which markedly increased the product yield, whereas non-cross-linked tiles resulted a nonspecific broken structure. 8-MOP is one in the library of irreversible cross-linkers available and a better cross-linker in terms of performance may be explored. To the best of our knowledge, this is the first report on the stability of self-assembled DNA origami structures that are nondegradable at higher-temperature. We anticipate that these stable structures will be useful for various applications such as nanoscale electronic and photonic devices, and higher-temperature assembly of functional molecules on origami surface.

■ ASSOCIATED CONTENT

Supporting Information. Materials and methods, the design of the tiles, and additional AFM images. This material is available free of charge via the Internet at http://pubs.acs.org.

■ AUTHOR INFORMATION

Corresponding Author
endo@kuchem.kyoto-u.ac.jp; hs@kuchem.kyoto-u.ac.jp

■ ACKNOWLEDGMENT

This work was supported by the CREST grant from the Japan Science and Technology Corporation (JST), grants for the WPI program (iCeMS, Kyoto University) and global COE program from the Ministry of Education, Culture, Sports, Science and Technology (MEXT). We thank Dr. Eiji Nakata and Prof. Takashi Morii for providing instrumentations. We extend our acknowledgement to Prof. Steven E. Rokita for supplying bisQMP and Mrs. Sekar Latha for her help with the graphics.

■ REFERENCES

(1) Rothemund, P. W. K. *Nature* **2006**, *440*, 297.
(2) (a) Andersen, E. S.; Dong, M.; Nielsen, M. M.; Jahn, K.; Subramani, R.; Mamdouh, W.; Golas, M. M.; Sander, B.; Stark, H.; Oliveira, C. L. P.; Pedersen, J. S.; Birkedal, V.; Besenbacher, F.; Gothelf, K. V.; Kjems, J. *Nature* **2009**, *459*, 73. (b) Douglas, S. M.; Dietz, H.; Liedl, T.; Hogberg, B.; Graf, F.; Shih, W. M. *Nature* **2009**, *459*, 414. (c) Endo, M.; Hidaka, K.; Kato, T.; Namba, K.; Sugiyama, H. *J. Am. Chem. Soc.* **2009**, *131*, 15570. (d) Endo, M.; Hidaka, K.; Sugiyama, H. *Org. Biomol. Chem.* **2011**, *9*, 2075.
(3) (a) Zhao, Z.; Yan, H.; Liu, Y. *Angew. Chem., Int. Ed.* **2010**, *49*, 1414. (b) Rajendran, A.; Endo, M.; Katsuda, Y.; Hidaka, K.; Sugiyama, H. *ACS Nano* **2011**, *5*, 665. (c) Liu, W.; Zhong, H.; Wang, R.; Seeman, N. C. *Angew. Chem., Int. Ed.* **2010**, *50*, 264. (d) Endo, M.; Sugita, T.; Rajendran, A.; Katsuda, Y.; Emura, T.; Hidaka, K.; Sugiyama, H. *Chem. Commun.* **2011**, *47*, 3213.
(4) (a) Chhabra, R.; Sharma, J.; Ke, Y.; Liu, Y.; Rinker, S.; Lindsay, S.; Yan, H. *J. Am. Chem. Soc.* **2007**, *129*, 10304. (b) Ding, B.; Deng, Z.; Yan, H.; Cabrini, S.; Zuckermann, R. N.; Bokor, J. *J. Am. Chem. Soc.* **2010**, *132*, 3248. (c) Shen, W.; Zhong, H.; Neff, D.; Norton, M. L. *J. Am. Chem. Soc.* **2009**, *131*, 6660. (d) Maune, H. T.; Han, S.; Barish, R. D.; Bockrath, M.; Goddard, W. A., III.; Rothemund, P. W. K.; Winfree, E. *Nat. Nanotechnol.* **2010**, *5*, 61. (e) Numajiri, K.; Kimura, M.; Kuzuya, A.; Komiyama, M. *Chem. Commun.* **2010**, *46*, 5127.
(5) Douglas, S. M.; Chou, J. J.; Shih, W. M. *Proc. Natl. Acad. Sci. U.S. A.* **2007**, *104*, 6644.
(6) (a) Endo, M.; Katsuda, Y.; Hidaka, K.; Sugiyama, H. *J. Am. Chem. Soc.* **2010**, *132*, 1592. (b) Endo, M.; Katsuda, Y.; Hidaka, K.; Sugiyama, H. *Angew. Chem., Int. Ed.* **2010**, *49*, 9412.
(7) (a) Sannohe, Y.; Endo, M.; Katsuda, Y.; Hidaka, K.; Sugiyama, H. *J. Am. Chem. Soc.* **2010**, *132*, 16311. (b) Subramani, R.; Juul, S.; Rotaru, A.; Andersen, F. F.; Gothelf, K. V.; Mamdouh, W.; Besenbacher, F.; Dong, M.; Kundsen, B. R. *ACS Nano* **2010**, *4*, 5969.
(8) Rajendran, A.; Endo, M.; Sugiyama, H. *Angew. Chem., Int. Ed.* **2011**in press.
(9) (a) Kershner, R. J.; Bozano, L. D.; Micheel, C. M.; Hung, A. M.; Fornof, A. R.; Cha, J. N.; Rettner, C. T.; Bersani, M.; Frommer, J.; Rothemund, P. W. K.; Wallraff, G. M. *Nat. Nanotechnol.* **2009**, *4*, 557. (b) Hung, A. M.; Micheel, C. M.; Bozano, L. D.; Osterbur, L. W.; Wallraff, G. M.; Cha, J. N. *Nat. Nanotechnol.* **2010**, *5*, 121.
(10) Castro, C. E.; Kilchherr, F.; Kim, D.-N.; Shiao, E. L.; Wauer, T.; Wortmann, P.; Bathe, M.; Dietz, H. *Nat. Methods* **2011**, *8*, 221.
(11) Mei, Q.; Wei, X.; Su, F.; Liu, Y.; Youngbull, C.; Johnson, R.; Lindsay, S.; Yan, H.; Meldrum, D. *Nano Lett.* **2011**, *11*, 1477.
(12) Higgins, N. P.; Cozzarelli, N. R. *Methods Enzymol.* **1979**, *68*, 50.
(13) Tagawa, M.; Shohda, K.; Fujimoto, K.; Sugawara, T.; Suyama, A. *Nucleic Acids Res.* **2007**, *35*, e140.
(14) (a) Hofr, C.; Brabec, V. *J. Biol. Chem.* **2001**, *276*, 9655. (b) Rajendran, A.; Magesh, C. J.; Perumal, P. T. *Biochim. Biophys. Acta* **2008**, *1780*, 282.
(15) Cleaver, J. E.; Killpack, S.; Gruenert, D. C. *Environ. Health Perspect.* **1985**, *62*, 127.
(16) (a) El-Mofty, A. M.; El-sawalhy, H.; El-Mofty, M. *Int. J. Dermatol.* **1994**, *33*, 588. (b) Cimino, G. D.; Gamper, H. B.; Isaacs, S. T.; Hearst, J. E. *Annu. Rev. Biochem.* **1985**, *54*, 1151. (c) Sastry, S. S.; Ross, B. M.; Parraga, A. *J. Biol. Chem.* **1997**, *272*, 3715. (d) Derheimer, F. A.; Hicks, J. K.; Paulsen, M. T.; Canman, C. E.; Ljungman, M. *Mol. Pharmacol.* **2009**, *75*, 599. Also ref 20.
(17) Endo, M.; Sugita, T.; Katsuda, Y.; Hidaka, K.; Sugiyama, H. *Chem.—Eur. J.* **2010**, *16*, 5362.
(18) (a) Anderson, T. F.; Voorhees, J. J. *Annu. Rev. Pharmacol. Toxicol.* **1980**, *20*, 235. (b) Kim, S. H.; Peckler, S.; Graves, B.; Kanne, D.; Rapoport, H.; Hearst, J. E. *Cold Spring Harbor Symp. Quant. Biol.* **1983**, *47*, 361. (c) Cao, H.; Hearst, J. E.; Corash, L.; Wang, Y. *Anal. Chem.* **2008**, *80*, 2932.
(19) Wang., H.; Rokita, S. E. *Angew. Chem., Int. Ed.* **2010**, *49*, 5957.
(20) Smith, S. I.; Brodbelt, J. S. *Analyst* **2010**, *135*, 943.